

# Dwarf 88, a novel putative esterase gene affecting architecture of rice plant

Zhenyu Gao · Qian Qian · Xiaohui Liu ·  
Meixian Yan · Qi Feng · Guojun Dong ·  
Jian Liu · Bin Han

Received: 5 May 2009 / Accepted: 30 June 2009 / Published online: 15 July 2009  
© Springer Science+Business Media B.V. 2009

**Abstract** Rice architecture is an important agronomic trait that affects grain yield. We characterized a tillering dwarf mutant *d88* derived from *Oryza sativa* ssp. *japonica* cultivar Lansheng treated with EMS. The mutant had excessive shorter tillers and smaller panicles and seeds compared to the wild-type. A reduction in number and size of parenchyma cells around stem marrow cavity as well as a delay in the elongation of parenchyma cells caused slender tillers and dwarfism in the *d88* mutant. The *D88* gene was isolated via map-based cloning and identified to encode a putative esterase. The gene was expressed in most rice organs, with especially high levels in the vascular tissues. The mutant carried a nucleotide substitution in the first exon of the gene that led to the substitution of arginine for glycine, which presumably disrupted the functionally conserved *N*-myristoylation domain of the protein. The function of the gene was confirmed by complementation test and antisense analysis. *D88*, thus, represents a new category of genes that regulates cell growth and organ development and consequently plant architecture. The potential relationship between the tiller formation

associated genes and *D88* is discussed and future identification of the substrate for *D88* may lead to the characterization of new pathways regulating plant development.

**Keywords** Rice · Tillering dwarf · *D88* · Esterase · Map-based cloning

## Abbreviations

CAPS	Cleaved amplified polymorphic sequences
CDAP	Cell death associated protein
<i>d88</i>	<i>dwarf 88</i>
EMS	Ethyl methane sulfonate
FAA	Formalin–acetic acid–alcohol
<i>FC1</i>	<i>FINE CULM 1</i>
GA	Gibberellic acid
LRR	Leucine rich repeat
<i>moc1</i>	<i>Mono culm 1</i>
ORFs	Open reading frames
OsCCD8	<i>Oryza sativa</i> carotenoid cleavage dioxygenase 8
PCR	Polymerase chain reaction
PME	Pectin methyl esterase
RT	Reverse transcriptase
SD	Standard deviation
SSR	Simple sequence repeat
STS	Sequence tagged site
<i>TB1</i>	<i>TEOSINTE BRANCHED 1</i>

**Electronic supplementary material** The online version of this article (doi:10.1007/s11103-009-9522-x) contains supplementary material, which is available to authorized users.

Z. Gao · X. Liu · Q. Feng · B. Han (✉)  
National Center for Gene Research/Institute of Plant Physiology  
and Ecology, Shanghai Institutes for Biological Sciences,  
Chinese Academy of Sciences, 500 Caobao Road, 200233  
Shanghai, China  
e-mail: bhan@ncgr.ac.cn

Z. Gao · Q. Qian (✉) · M. Yan · G. Dong · J. Liu  
State Key Laboratory of Rice Biology, China National Rice  
Research Institute, Chinese Academy of Agricultural Sciences,  
310006 Hangzhou, China  
e-mail: qianqian188@hotmail.com

## Introduction

Plant height and branching behavior are important agronomic traits affecting crop yield. Types of branching patterns characterized during rice plant development include the initiation of tillers from axillary buds at the phase of vegetative growth and branching of inflorescence that

determines the number of spikelets born on each tiller. Substantial progress was made recently toward identification of the molecular developmental control of rice tillering (Wang and Li 2008). It was shown that rice *FCI* was an ortholog of *TBI* in maize (Takeda et al. 2003), a repressor of axillary bud growth (Hubbard et al. 2002). The study on *moc1* mutant, which had only the main culm without tillers, identified *MOC1* encoding a GRAS transcription factor as a critical switch during axillary meristem development (Li et al. 2003).

A group of rice dwarf mutants, tillering dwarf mutants, with a large number of short tillers is particularly valuable for further characterizing the molecular basis for the establishment of plant architecture (Ward and Leyser 2004). Six tillering dwarf mutants of rice have been reported, including *bunketsuwaito tillering dwarf (d3)*, *toyohikaribunwai tillering dwarf (d10)*, *kamikawabunwai tillering dwarf (d14)*, *slender dwarf (d17)*, *bunketsuto tillering dwarf (d27)* and *bonsaito dwarf (d33)* (Ishikawa et al. 2005), of which genes underlying *d3*, *d10*, *d17* and *d27* have been cloned. The *D3* gene encodes a protein orthologous to *Arabidopsis* MAX2, a member of the F-box LRR family that functions as a component of the ubiquitin E3 ligase complex. The insertion of a putative transposon into *D3* caused an alteration of the amino acid sequence and generated a premature stop codon (Ishikawa et al. 2005). The *D10* gene is a rice ortholog of *MAX4/RMS1/DAD1* that encodes an OsCCD8, supposedly involved in the synthesis of an unidentified inhibitor of shoot branching (Arite et al. 2007). *D17*, or *HTD1*, responsible for high tillering dwarf phenotypes in the *htd1* mutant, codes for an ortholog of *Arabidopsis* MAX3, required for the negative regulation of axillary bud outgrowth (Zou et al. 2006). More recently, *D27*, encodes a novel iron-containing protein required for the biosynthesis of a new class of phytohormones, Strigolactones, was isolated via map-based cloning (Lin et al. 2009).

In this study, we characterized a rice mutant, designated as *d88*, found to be allelic to *d14*. Both allelic mutants exhibited reduced plant height, a larger number of tillers, and smaller seeds compared to the wild-types. We then cloned the *D88* gene using a map-based cloning strategy, which encodes a novel putative rice esterase. A nucleotide substitution leading to an amino acid substitution in *d88* and a transposon insertion in *d14* resulted in mutant phenotypes.

## Materials and methods

### Plant materials and growth conditions

The rice *tillering dwarf* mutant, *d88*, was isolated from *Oryza sativa* ssp. *Japonica* cultivar Lansheng treated with

EMS. The *d3*, *d10*, *d14*, *d27* mutant and the wild-type Shiokari were kindly provided by Dr. Takamura at Hokkaido University in Japan. In this study, we also generated *d88-Shiokari* mutants by backcrossing the *d88* mutant plants with *japonica* variety Shiokari. To generate a large F<sub>2</sub> mapping population, *d88* was crossed with an *indica* cultivar, Nanjing 6. Rice plants were grown in the experimental field at the China National Rice Research Institute. Plant height was measured from the base of the shoot to the tip of the longest leaf before heading, and at mature stage from the base of the shoot to the tip of the longest panicle.

### Genetic analysis, sequence analysis and phylogenetic analysis

The rice genomic DNA preparation was performed as described (Qian et al. 2001). To fine-map the *D88* locus, new molecular markers, including the SSR, STS and CAPS markers, were developed (Table 1). The genetic linkage between the *D88* locus and molecular markers was determined using Mapmaker 3.0 (Lander et al. 1987).

The entire genomic region spanning *D88* locus was amplified for the mutants (*d88* and *d14*) and their corresponding wild-type plants by PCR with LA-Taq (TaKaRa). The PCR program included 4 min at 94°C, followed by 30 cycles of 94°C for 1 min, 60°C for 1 min, and 72°C for 3.5 min, and a final extension at 72°C for 10 min. PCR products were sequenced directly, and the mutations in *d88* and *d14* were identified and verified further by sequencing two additional independent PCR products. Sequencing was performed using BigDye terminator v3.1 (ABI 9600). The mutation in *d88* also can be detected by restriction analysis with BsmF I.

Gene prediction was performed using Rice Genome Automated Annotation system (RiceGAAS, <http://ricegaas.dna.affrc.go.jp/>), and intron/exon structures were verified by alignment of the cDNA sequence of rice with the genomic DNA sequence. Multiple sequence alignments were conducted using CLUSTAL W 1.8 with the PAM matrix. A UPGMA tree (Saitou and Nei 1987) was built using MEGA 3.1 adopting Poisson correction distance, and the tree was presented using TreeView (Page 1996). Support for the tree obtained was assessed using the bootstrap method (Felsenstein 1985) and the number of replicates was 100.

### Construction of vectors and plant transformation

A 5.64-kb genomic DNA fragment isolated from *Bam*HI digested BAC clone AC104429 (OSJNBb0006P09) containing the entire esterase gene, the 2,770-bp upstream sequence, and the 1,829-bp downstream sequence was inserted into the binary vector pCAMBIA1300 to generate the transformation plasmid pCAMBIA1300-*Est* for the

**Table 1** List of the PCR-based molecular markers developed in this study

Marker	Primer pairs	Restriction enzyme
P3-1	F, 5'-CTCCTTCGCCGCTCTCCTC-3'; R, 5'-TGGAGCGAGAGCACGAGGTC-3'	
P3-2	F, 5'-CACAGGAGATCAGAGGCTCAC-3'; R, 5'-TGCATACGCTACAGGACACG-3'	BstUI
P3-3	F, 5'-CCAGATCTACTACCTCCATTAGAC-3'; R, 5'-CAAGATATGTTTCAGATACAGTTCAC-3'	
P3-4	F, 5'-CGGTAGCAGCTAAGCGATG-3'; R, 5'-GAGCATAGGAATCTCTCAGCAAG-3'	
P3-5	F, 5'-GAAAGACGACACATGGCGA-3'; R, 5'-ATTCGTTGTTGGCGTAGTGG-3'	Sau3AI
P3-6	F, 5'-CGACTAAAGCGATGTCAGTAAGA-3'; R, 5'-TCCGTATGGCAGGAACAAC-3'	
P3-7	F, 5'-TTACACGTCTGCTGCAAGTCTG-3'; R, 5'-CCATGCTCAACTGCAATGTGT-3'	BstUI
P3-8	F, 5'-GATCAACCGCCGTGTGACAAG-3'; R, 5'-CAGTTCACCGCTGTACGTTGCT-3'	AvaI
P3-9	F, 5'-CCATGTTGAATATCATCACCA-3'; R, 5'-TCCTTGTTCATCGTCATTGTAG-3'	XhoI
P3-10	F, 5'-AAGCCTTCTTACCGACTCTC-3'; R, 5'-GTGAGCAGTGTCCAAGTCC-3'	

F forward primer, R reverse primer

complementation test (Fig. 5a). pCAMBIA1300 was transformed as a control. The two binary plasmids were introduced into *Agrobacterium tumefaciens* EHA105 by electroperation, and calli of the *d88* mutant were transformed according to a published method (Hiei et al. 1994). HygF (5'-GGAGCATATACGCCCGGAGT-3') and HygR (5'-GTTTATCGGCACTTTGCATCG-3') for hygromycin resistance were applied for transgenic plants screening. For antisense analysis, the rice variety Nipponbare was transformed with pCAMBIA-*Ubi-Estanti*, which contains the reverse sequence of nucleotide 87–417 of the esterase gene amplified with DAF (5'-TCGGCGTCGTCGAGCTCG GAGAAG-3') and DAR (5'-CAGCCCGGGATGCGGAG CGCGTC-3') (Fig. 5b). DAF-2 (5'-GCTCGGAGAAGAC GATGGTG-3') and UbiF (5'-TAGCCCTGCCTTCATA CGC-3') were used for detection of transformants. A 1.565-kb promoter region of the *D88* gene was amplified by high fidelity PCR using forward primer 5'-TTGGTACCT ACTTGAAACTATGTTGAGCA-3' and reverse primer 5'-TTAGATCTACCATCACACCAGCGCGGC-3', and then inserted upstream of the 5' end of the *uidA* gene encoding  $\beta$ -glucuronidase (GUS) in pCAMBIA1301 to create a pD88:GUS fusion construct vector and transformed into Nipponbare via *Agrobacterium tumefaciens*.

#### RT-PCR analysis

Total RNA was extracted from leaves, culms, roots, flowers at mature stage, and stem base (a segment of

approximately 5 mm containing the unelongated internodes) from 4-leaf stage seedlings according to the method described by Wadsworth et al. (1988). For RT-PCR, first-strand cDNA was transcribed reversibly from total RNA with oligo(dT)<sub>16</sub> as the primer using SuperScriptII (Invitrogen) and used as the template for PCR. Primers for *D88* were EcF and EcR (5'-ATGCTGCGATCGACGCATCC-3' and 5'-TTAGTACCGGCGAGAGCG-3'), for *HTD1* were HTD1F and HTD1R (5'-GAGGATGGTGGCTATGTTCTTCT-3' and 5'-AGTAGTTATTTGGTTCCTCCCTGAT-3'), for *OSHI* were OSH1F and OSH1R (5'-GAGATTGAT GCACATGGTGTG-3' and 5'-ATTAGCAGCAGCAAGA GTAGC-3'), for *D3* were D3F and D3R (5'-CTGGCC TCTAGAAGGAGTAGATTAGGTAG-3' and 5'-CTGAT GAAGAGAAACCAGGGAAAAC-3'), for *D10* were D10F and D10R (5'-GGTAGCAACGAGAGGCAGTT-3' and 5'-TCGACCTTGGTGAGCGTGT-3'), and those for *Actin* (control) were ActF and ActR (5'-TCATGAAGA TCCTGACGGAG-3' and 5'-AACAGCTCCTCTTGCT TAG-3'). For real time PCR (ABI 7500), *D88* primers were Ec-2F and Ec-2R (5'-CGCCTTCGTCGGCCACTC-3' and 5'-TCGAACCCGCGTGGTAGTC-3'), *Actin* primers were ACTINF and ACTINR (5'-GGTCGTACCCAAGG TAATGTGT-3' and 5'-CTCCATTTCTGGTCATAGTCC-3').

#### Histological analysis and GUS assay

Plant materials (5 mm sections from main stem base of 4-leaf stage seedlings) fixed in FAA were dehydrated through

a graded ethanol series and embedded in Paraplast Plus. Microtome sections (1–2  $\mu\text{m}$  thick) stained with toluidine blue was observed and photographed under a microscope with a digital color camera (Olympus AX70).

Histochemical GUS analysis was performed as described with minor modifications (Jefferson et al. 1987). Transgenic plant samples were incubated in X-gluc buffer overnight at 37°C. The stained tissues were observed and photographed using a stereomicroscope with a camera (Nikon SMZ1000). Leaves were then destained in 70% (w/v) ethanol. After being stained with X-gluc, the tissues were rinsed and fixed in FAA fixation solution at 4°C overnight. After dehydration with graded ethanol and replacement of ethanol with xylol, the tissues were embedded in paraffin and then sectioned with a microtome (HM315R). Sections of 5–8  $\mu\text{m}$  thick were mounted on slides, and observed and photographed under a microscope (Olympus AX70).

## Results

### Phenotypes of the *d88* mutant

To determine the relation of *d88* with previously isolated tillering dwarf mutants, we crossed *d88* with the following mutants: *d3*, *d10*, *d14* and *d27*. We found that clear segregation of the phenotypes existed in the F<sub>2</sub> generation of the mutants expect for *d14*. All nice F<sub>1</sub> plants of *d14/d88* exhibited tillering dwarf phenotype (plant height = 37.0  $\pm$  4.6 cm, tiller number = 54.9  $\pm$  9.6, mean  $\pm$  SD,  $n$  = 9;  $t$ -test:  $P$  > 0.05) and no segregation was found in F<sub>2</sub> (plant height = 36.7  $\pm$  5.0 cm, tiller number = 55.0  $\pm$  11.0, mean  $\pm$  SD,  $n$  = 30, 6 F<sub>2</sub> plants from 5 F<sub>1</sub> lines;  $t$ -test:  $P$  > 0.05). Morphologically, *d88* and *d14* are distinguishable from wild-type Lansheng and Shiokari, respectively. When we quantitatively compared *d88* and *d14* with their wild-type plants concerning plant height, tiller number and seed weight, both mutants produced larger number of shorter tillers with smaller sizes of panicles and seeds in comparison to the wild-types (Table 2; Fig. 1). Tiller bud

had emerged at 3-leaf stage in *d88* and *d14*, while no bud could be seen in their wild-type plants (Data not shown).

Observation showed the main culm of *d88* elongated more slowly than that of the Lansheng wild-type soon after germination and reached about only less than 30% of Lansheng in plant height after heading, whereas *d14* displayed shorter main culm than the Shiokari wild-type approximately 20 days after germination (Supplementary Fig. 1a). According to the classification scheme of rice dwarf mutants (Takeda 1977), the panicle and the upper four internodes of the *d88* and *d14* mutants were measured and compared with those of the wild-type, Lansheng and Shiokari, respectively. As shown in Table 2 and Supplementary Fig. 1b, both mutants belong to the dn-type of dwarfism, i.e., showing average shortening of each internode except for the fourth internode in *d14*.

Microscopic observation showed that the number of collenchyma cell layers under epidermis and the number of parenchyma cell layers around marrow cavity in *d88* are not different from those in the Lansheng wild-type. However, the number and the size of parenchyma cells per layer decreased in *d88*, as well as the smaller volume of marrow cavity with delayed development of vascular bundle, which resulted in the reduction in tiller diameter by about half of the wild-type (Fig. 2a, b). Elongation of parenchyma cells retarded markedly at early stage in *d88*, which contributed to the dwarfism of the mutant (Fig. 2c, d).

### Positional cloning of the *D88* gene

We demonstrated that *d88* was controlled genetically by a single locus based on the segregation ratio that 338 out of 1,378 F<sub>2</sub> plants derived from a cross between *d88* and Nanjing 6 showed the mutant phenotype ( $\chi^2 = 0.164$ ,  $0.50 < P < 0.75$ ). Using this population, the locus was mapped between SSR markers, RM5480 and RM5442, on the short arm of rice chromosome 3 (Fig. 3a). We further generated a larger F<sub>2</sub> mapping population with 708 homozygous recessive plants and fine-mapped the locus between SSR markers, P3-1 and P3-10, which corresponded to sequences on a single BAC, OSJNBb0006P09 of the

**Table 2** Comparison of traits of Lansheng and *d88*, Shiokari and *d14*

Trait	Lansheng <sup>a</sup>	<i>d88</i> <sup>a</sup>	Shiokari <sup>a</sup>	<i>d14</i> <sup>a</sup>
Plant height (cm)	100.5 $\pm$ 5.3	32.5 $\pm$ 3.5**	56.5 $\pm$ 0.7	32.1 $\pm$ 2.7**
Panicle length (cm)	21.8 $\pm$ 1.0	9.0 $\pm$ 1.4**	13.0 $\pm$ 0.3	6.8 $\pm$ 0.1**
First internode length (cm)	38.2 $\pm$ 4.1	10.9 $\pm$ 1.0**	20.4 $\pm$ 3.7	14.5 $\pm$ 1.6**
Second internode length (cm)	23.0 $\pm$ 3.5	6.1 $\pm$ 1.3**	12.9 $\pm$ 2.8	4.6 $\pm$ 0.2**
Third internode length (cm)	10.8 $\pm$ 1.2	4.8 $\pm$ 0.4**	6.6 $\pm$ 0.8	1.6 $\pm$ 0.6**
Fourth internode length (cm)	4.1 $\pm$ 0.7	1.9 $\pm$ 0.1**	1.1 $\pm$ 0.0	1.2 $\pm$ 0.3
Tiller number	10.0 $\pm$ 2.0	56.0 $\pm$ 4.2**	29.0 $\pm$ 0.0	64.0 $\pm$ 5.1**
1,000 seeds weight (g)	33.2 $\pm$ 0.5	18.3 $\pm$ 0.5**	24.0 $\pm$ 0.4	17.7 $\pm$ 0.3**

\*\* Represent the significance of difference at the 0.01 level

<sup>a</sup> Mean  $\pm$  SD with 5 replicates

**Fig. 1** Phenotypes of Lansheng, *d88*, Shiokari, *d14* at mature stage. **a** and **b** Plants, Scale bars = 5 cm. **c** and **d** Seeds, Scale bars = 5 mm. **e** and **f** Panicles, Scale bars = 5 cm

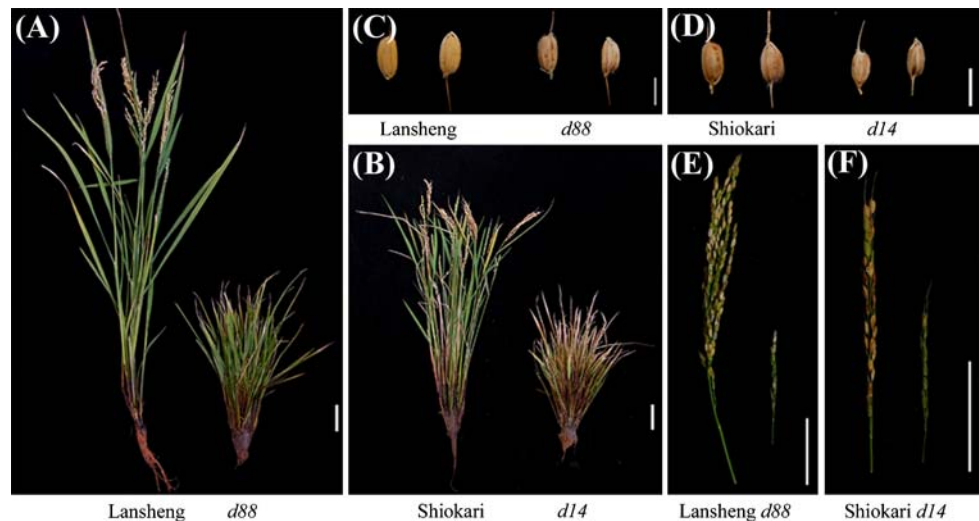
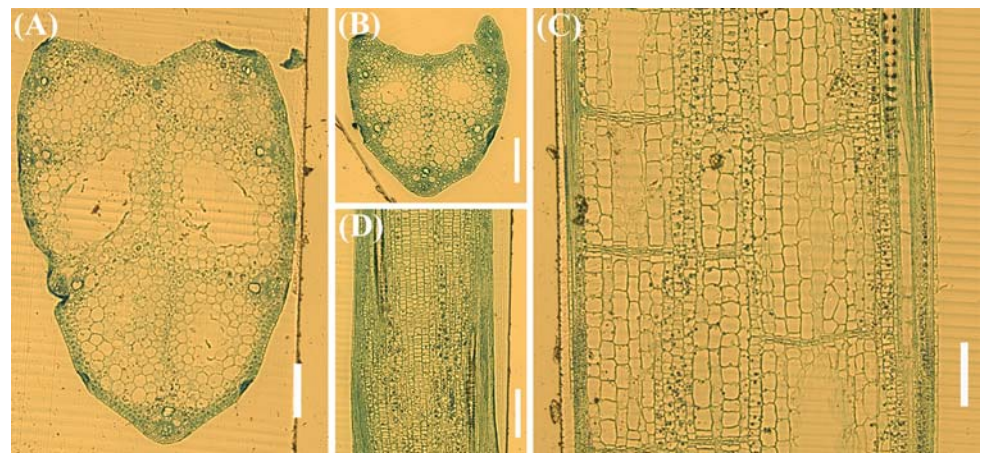


**Fig. 2** Microstructure of main stem base of Lansheng (**a**, **c**) and *d88* (**b**, **d**) at 4-leaf stage (200 multiple). **a** Transversal section of Lansheng. **b** Transversal section of *d88*. **c** Longitudinal section of Lansheng. **d** Longitudinal section of *d88*. Scale bars = 0.1 mm



Nipponbare genome sequences (Fig. 3b). To further narrow down the locus, we developed eight additional markers according to the genome sequences, and mapped the *D88* gene within an interval of 14.5-kb between markers, P3-2 and P3-4 (Fig. 3c). In this region, Five ORFs were predicted including three hypothetical proteins, a hypothetical retrotransposon protein and a putative esterase harboring  $\alpha/\beta$  hydrolase fold (Fig. 3d).

#### *D88* encodes a putative esterase

The genomic DNA sequences from *d88* corresponding to the putative esterase gene and other four hypothetical genes were PCR amplified and sequenced. Comparison of the sequences of the Lansheng wild-type and *d88* revealed that the *d88* allele carries a single nucleotide substitution in nucleotide 235 (GGG → AGG) in the first exon of the esterase gene, which changes glycine into arginine, disrupting the N-myristoylation site in the protein. No sequence difference of other four genes was found between

the mutant and the wild-type, thus suggested that the esterase gene was more likely the candidate.

We then compared the sequences of the esterase gene between *d14* and the wild-type Shiokari. The mutant was found contained a 615-bp insertion with 19-bp terminal inverted repeats flanked by direct repeats GGGCGAT in the intron between the two exon of the esterase gene (Fig. 3e). The study of expression of the gene in *d14* showed that its expression was substantially reduced to the level that the RT-PCR product was barely visualized on the gel (Supplementary Fig. 2a). Therefore, the esterase was considered to be the candidate for *D88*.

For further exploring the association between the presence of this amino acid change in *D88* and abnormal phenotypes of *d88*, the substitution in the *d88* allele, disrupting the BsmF I site in the genomic DNA, can be used as a CAPS marker to examine the distribution of this nucleotide substitution among different rice varieties including normal and semi-dwarf varieties (Data not shown). Our association analysis of the specific amino acid

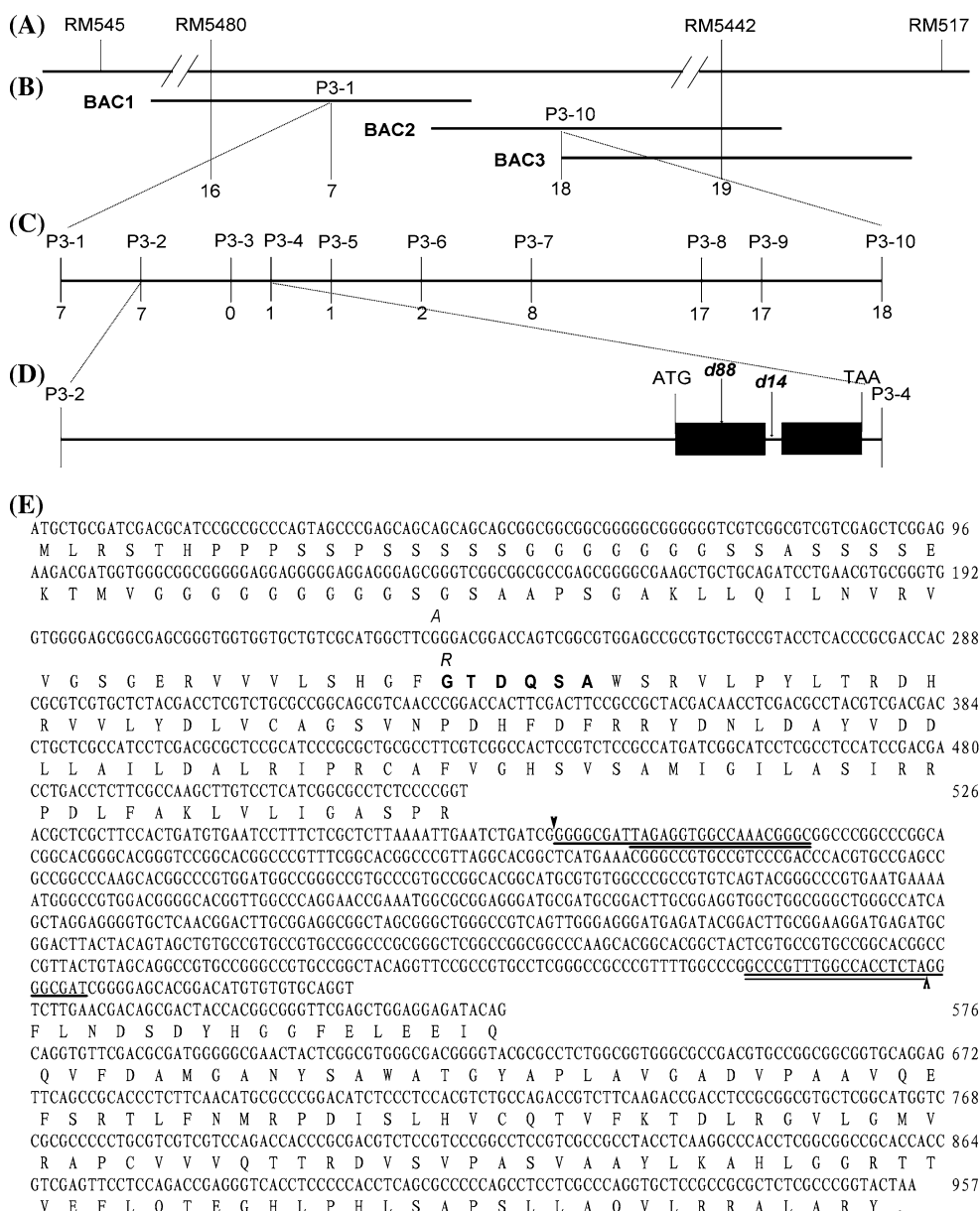


**Fig. 3** Fine mapping and positional cloning of the *D88* gene. **a** The *D88* locus was mapped on the chromosome 3 between markers, RM5480 and RM5442. **b** Three-BAC contig covering the *D88* locus. The numerals indicate the number of recombinants identified from 708 recessive F<sub>2</sub> plants. BAC1: AC104429; BAC2: AC123568; BAC3: AC132214. **c** Fine mapping of the *D88* locus with the markers (P3-2 to P3-9) developed based on the OSJNBb0006P09 sequence. The *D88* locus was narrowed to a 14.5-kb genomic DNA region between CAPS marker P3-2 and STS marker P3-4. **d** *D88* gene (ORF5) structure with the mutated sites of the two alleles and other four ORFs. The start codon (ATG) and the stop codon (TAA/TAG/

TGA) are indicated. Closed boxes indicate the coding sequence, and line between boxes indicates intron. Mutation sites in *d88* and *d14* are also shown with vertical arrows. **e** *D88* gDNA, cDNA and predicted amino acid sequences. Numbers for cDNA sequence are listed on the right side. *Italic letters* indicate the 1-bp or an amino acid substitution in *d88*; Sequence between two arrow heads is a 615-bp insertion in *d14*, which inserted into the intron without amino acid sequence below. *Letters underlined* indicate the direct 8-nucleotide repeats, *double underlined* 19-bp terminal inverted repeats. *Bold letters* indicate the conserved N-myristoylation site

change in *D88* with abnormal phenotypes of the *d88* mutant indicates that the glycine at this position is conserved in function across rice varieties. Therefore, the amino acid substitution at this position could confer phenotypic change such as that seen in *d88*.

To determine the evolutionary relationships of rice *D88* family, an unrooted tree was constructed using the UPGMA method (Fig. 4). Phylogenetic analysis indicated hydrolases from plant could be grouped into two clades, esterases/hydrolases/carboxylesterases and pectin

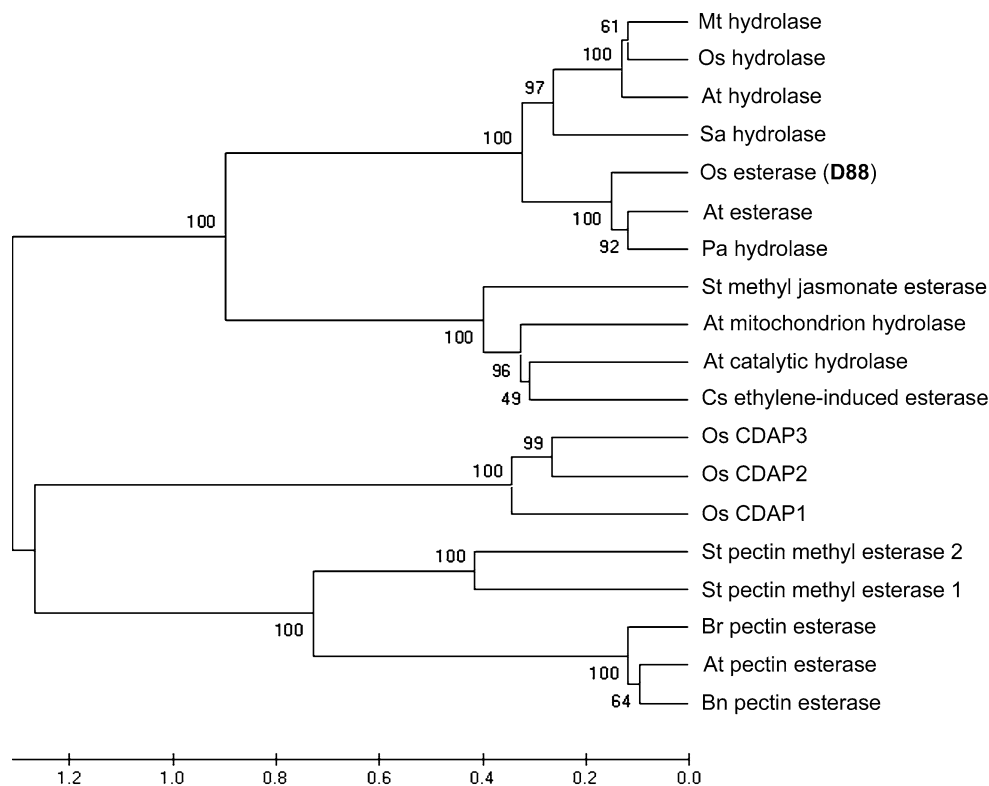


**Fig. 4** Phylogenetic relationship of D88 to other plant hydrolases. The GenBank accession numbers of the sequences used for the analysis are: Mt hydrolase, *Medicago truncatula* (barrel medic) ABE87031; Os hydrolase, *Oryza sativa* ABF96818; At hydrolase, *Arabidopsis thaliana* NP\_195463; Sa hydrolase, *Striga asiatica* ABD98032; Os esterase (D88), *Oryza sativa* ABF94526; At esterase, *Arabidopsis thaliana* NP\_566220; Pa hydrolase, *Platanus acerifolia* CAJ91149; St methyl jasmonate esterase, *Solanum tuberosum* (potato) AAV87151; At mitochondrion hydrolase, *Arabidopsis thaliana* NP\_195432; At catalytic hydrolase, *Arabidopsis thaliana* NP\_179942; Cs ethylene-induced

esterase, *Citrus sinensis* AAK58599; Os CDAP3, CDAP2, CDAP1, *Oryza sativa* NP\_911314, NP\_911312, NP\_911308; St pectin methyl esterase 2, *Solanum tuberosum* AAF23892; St pectin methyl esterase 1, *Solanum tuberosum* AAF23891; Br pectin esterase, *Brassica rapa* ssp. *pekinensis* AAB17084; At pectin esterase, *Arabidopsis thaliana* NP\_191776; Bn pectin esterase, *Brassica napus* (rape) CAA39658. The number at each node represents the bootstrap support (percentage). The scale bar is an indicator of genetic distance based on 0.2 amino acid substitutions per residue

esterases. The rice D88, belonged to the former clade in which gene divergence emerged before monocot and dicot diverge, had the highest homology (similarity index 75.1%) with *Platanus acerifolia* hydrolase involved in defence response to a product of the Ascomycete *Ceratocystis platani* (Fontana 2007), and then *Arabidopsis thaliana* esterase (GenBank accession number: NP\_566220, similarity index 73.8%), neither of which was related to branch development. Another gene for hydrolase with high similarity to D88 except N terminal was also mapped on chromosome 3 in rice (GenBank accession number: ABF96818).

The function of D88 was confirmed by a complementation test. The plasmid pCAMBIA1300-*Est* containing the entire gene (Fig. 5a) was introduced into the *d88* mutant, and four independent transgenic lines, DS1, DS2, DS3 and DS5 were obtained. Each transgenic line harbored one D88 transgene copy according to segregation analysis of T<sub>1</sub>

plants. All four lines with pCAMBIA1300-*Est* showed a complementation of the *d88* phenotype with normal tiller number and seed size although plant height was not fully restored (Supplementary Table 1; Fig. 5c, d). Antisense analysis with pCAMBIA-*Ubi-Estanti* obtained 5 of 15 independent transgenic lines mimicked the *d88* mutant phenotype, including increased tiller number and reduced plant height (Supplementary Table 1; Fig. 5e). The severity of the phenotype paralleled the degree of D88 expression (Fig. 5f, g). In most cases, the ratio of mutant-like and wild-type plants in T<sub>1</sub> generation was  $\approx$ 3:1.

#### Expression of D88 and tiller formation associated genes

As shown in Supplementary Fig. 2a, D88 was expressed in leaves, culms and roots, but at a very low level in flowers. The expression levels of D88 were similar between the *d88* mutant and the wild-type Lansheng, indicating that the

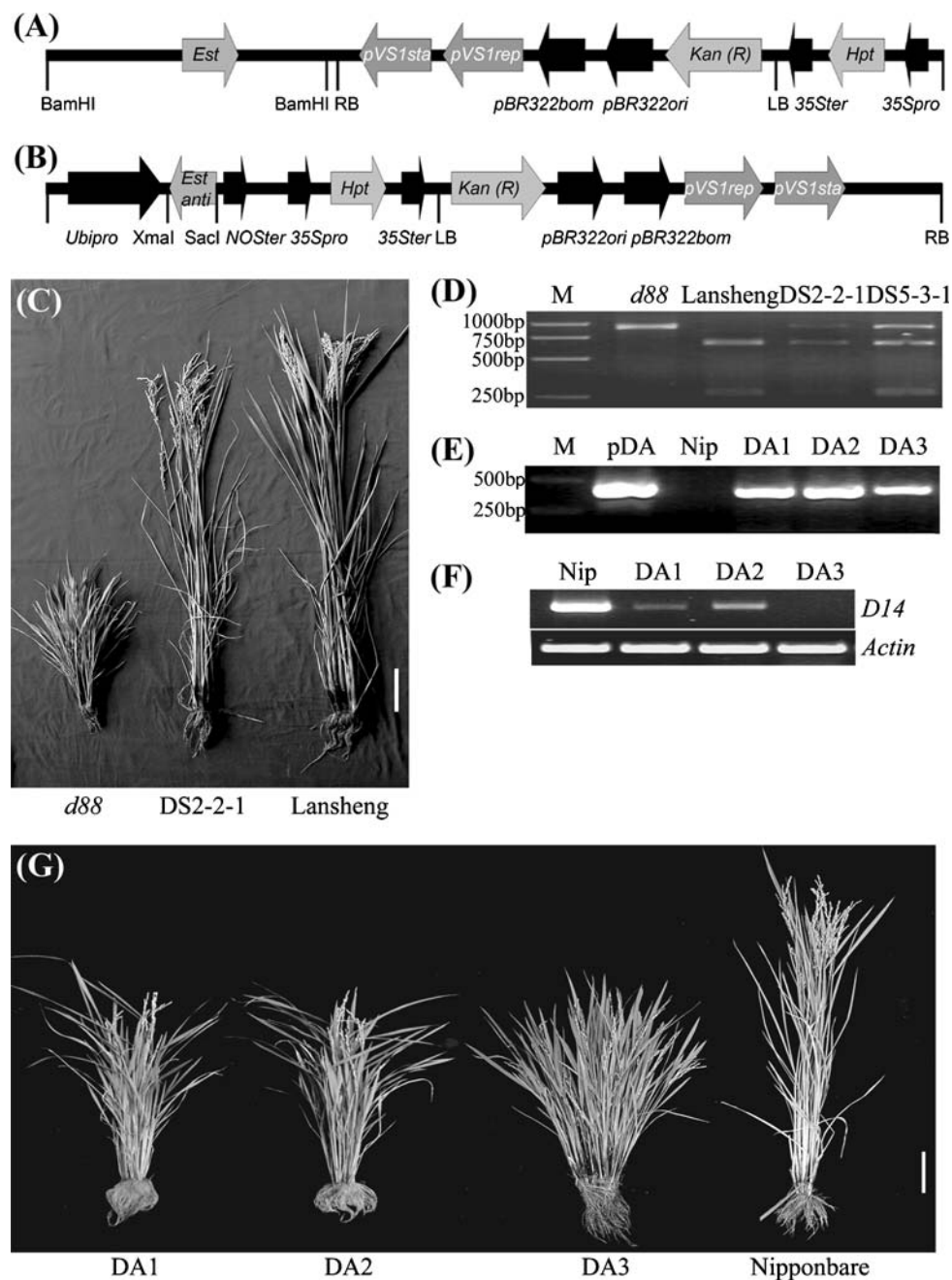


**Fig. 5** Complementation test and antisense analysis. **a** and **b** Schematic structure of the complementation construct pCAMBIA1300-*Est* and antisense construct pCAMBIA-*Ubi-Estanti*. pCAMBIA1300-*Est* contained the entire esterase gene, the 2,770-bp upstream sequence and the 1,829-bp downstream sequence; pCAMBIA-*Ubi-Estanti* contained reverse sequence of nucleotide 87–417 of the esterase gene. **c** The defects of the *d88* mutant were rescued by the introduction of pCAMBIA1300-*Est* though plant height was not restored completely. DS2-2-1 was the T<sub>2</sub> plant transformed with pCAMBIA1300-*Est*. Scale bar = 10 cm. **d–f** Molecular detection of transformed plants from complementation test and antisense analysis. **d** Identification of the transgenic plants with pCAMBIA1300-*Est*

using *d88* as a control. The G to A substitution in the *d88* allele disrupts an enzymatic site for BsmFI. M: DL2000 MARKER; DS2-2-1 and DS5-3-1 were transgenic T<sub>2</sub> plants with pCAMBIA1300-*Est*. **e** Identification of the transgenic plants with pCAMBIA-*Ubi-Estanti* using Nipponbare as a control. Primers DAF-2 and UbiF were used for PCR. M: DL2000 MARKER; pDA: pCAMBIA-*Ubi-Estanti*; Nip: Nipponbare; DA1, DA2 and DA3 were transgenic T<sub>0</sub> plants with pCAMBIA-*Ubi-Estanti*. **f** *D88* expression in culms of Nipponbare, DA1, DA2 and DA3. Nip: Nipponbare. *Actin* was amplified as control. **g** T<sub>0</sub> plants, DA1, DA2 and DA3 transformed with pCAMBIA-*Ubi-Estanti* exhibited typical *d88* phenotype compared with the recipient Nipponbare. Scale bar = 10 cm

base substitution affected only protein function. For the *d14* mutant, however, RT-PCR analysis revealed a dramatic reduction in the abundance of transcripts of 957-bp in comparison to the Shiokari wild-type (Supplementary Fig. 2a). Sequencing the 524-bp fragment indicated that it was a non-specific product (Data not shown). Real time PCR confirmed the expression of *D88* was reduced by more than 20 times in culms of *d14* in comparison to the Shiokari wild-type (Supplementary Table 2).

To further study the expression of *D88*, a binary vector containing the GUS gene driven by the *D88* promoter (*D88*:GUS) was constructed and used for rice transformation. Despite differences in the intensity of GUS activity, histochemical GUS staining of all 10 independently transgenic lines showed a common pattern of GUS distribution. As shown in Fig. 6m, n, consistent with the results of RT-PCR analysis, GUS staining was nearly undetectable in pistils or anthers despite weak staining on the glume ridges. Analyses with a longitudinal section and a transversal section of the root indicated that the GUS activity was localized mainly in the parenchyma cells in the root stele and lateral roots (Fig. 6c, e–g). A relatively high level of GUS expression was observed in the vascular tissues of vein and leaf sheath, ligule base, auricle base and stem base, especially in tiller buds (Fig. 6a, b, d, h–l).

To examine whether the expression of tiller formation associated genes were affected by the *D88* mutation, the expression of *HTD1*, *OSHI*, *D3* and *D10* were compared between the *d88* mutant and the Lansheng wild-type at the stem base of 4-leaf stage plants. The expression of *HTD1*, *OSHI* and *D10* increased significantly in the *d88* mutant compared to the wild-type, whereas that of *D3* remained unaltered in the mutant (Supplementary Fig. 2b).

*D88* may function through the MAX/RMS/D pathway

*D27* was proved to participate in the production of strigolactones, the novel hormones that inhibit plant branching derived from the MAX/RMS/D pathway in rice (Lin et al. 2009). The phenotype of *d88* and the independence of IAA (Data not shown) prompted us to test whether *D88* is a new member of the MAX/RMS/D pathway in rice. We therefore generated a *d88*-Shiokari *d27* double mutant and compared the phenotypes of single and double mutants of *d88*-Shiokari, *d27* and *d88*-Shiokari *d27*. As shown in Supplementary Fig. 3, *d88*-Shiokari exhibits similar phenotype to *d27*, but has fewer tillers and a more severe dwarf stature than *d27*. Phenotypic analysis revealed that the *d88*-Shiokari *d27* double mutant showed similar plant height to *d27*, and more tiller number than both mutants with large variation (Supplementary Fig. 3b, c). These results suggested that *D88* may be involved in the MAX/RMS/D pathway.

## Discussion

### Characteristics of rice *d*-type mutants

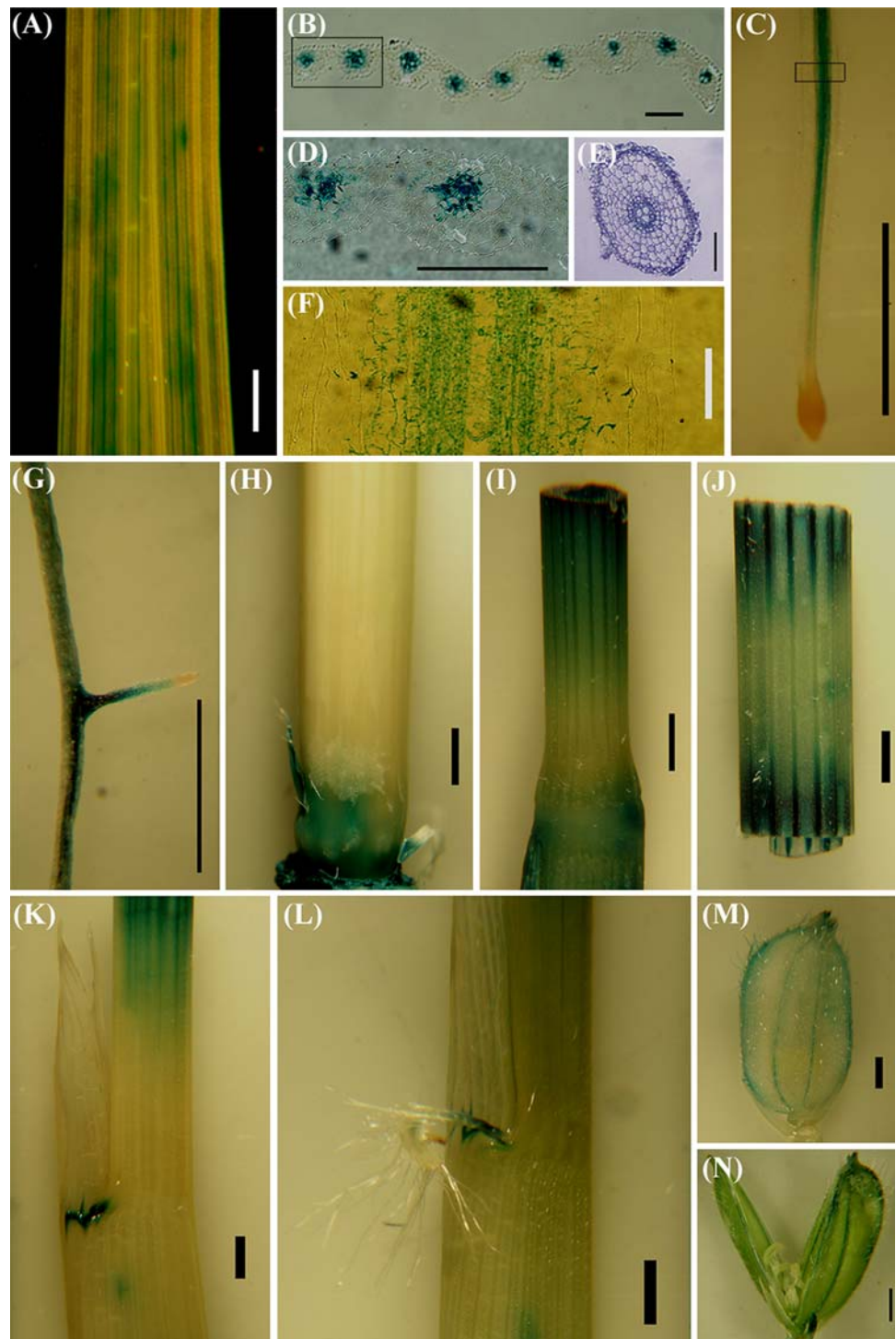
Five rice *d*-type mutants (*d3*, *d10*, *d14*, *d17* and *d27*) exhibited a similar abnormal appearance from the early stage of plant development. The most distinctive feature was a reduction of their stature as well as an increase in tiller number. Another mutant, *d33* had many tillers with narrow, rolled leaves (Kishimoto et al. 1992). The *htd-1* mutant (*d17*), mutated from Nanjing 6, presented milder defects with respect to plant height, and exhibited more excessive tillers than other *d* mutants. At the maturity stage, the number of tillers of *htd-1* is about nine times as many as that of Nanjing 6 (Zou et al. 2005). Our observation of *d88* and *d14* showed that both mutants had an increase in tiller number, reduction in culm length and grain size compared with their wild-types, in accordance with the result from Ishikawa et al. (2005) except for the decreased panicle size. In common, wild-type varieties increase their tiller numbers until the onsets of culm elongation and panicle initiation, and then the tiller number of each plant become immobile. Nevertheless, the *d88* and *d14* mutants still keep the high tillering capacity, although only one axillary bud in each leaf axil (data not shown). These observations suggest that the enhanced tillering capacity of the two allelic mutants result from the release of axillary buds from dormancy rather than from an increase in the number of axillary buds. Both allelic mutants belong to the dn-type of dwarfism as the *htd-1* mutant (Zou et al. 2005). In rice, stem elongation is caused by cell division in the meristem, followed by cell elongation in the cell elongation zone. Usually, dwarfing could be the result of a defect in one or both of the two processes. According to our observation, dwarfism in the *d88* mutant could be attributed to a defect in elongation of parenchyma cells.

Pleiotropism existed in *Arabidopsis bushy* mutant and in rice *tb1* mutant, in which the vascular system and flower development were hampered respectively (Reintanz et al. 2001; Takeda et al. 2003). Rice *D3* was also found involved in leaf senescence or cell death (Yan et al. 2007). Likewise, in addition to reduced plant height and far more tillers, *d88* and *d14* had shortened panicles, smaller seeds, and decreased seed set compared with their wild-types. Weak expression of the *D88* gene in ridges of glume hull revealed its effect on reproductive organ.

Mutation in *D88* affects expression of tiller formation associated genes

It is reasonable that transcriptional expression of *OSHI* dramatically enhanced in the *d88* mutant because with its

**Fig. 6** Localization of D88:GUS expression in a longitudinal section of a leaf (a), a root (c), a lateral root (g), a stem (h), a node and an internode (i), a leaf sheath (j), a ligule (k), an auricle (l), and an unpollinated flower (m, n), a transversal section of a leaf (b) and a root (e). (d) and (f) show closer views of the rectangle region in the leaf and root shown in (b) and (c). a, c, g–n Scale bars = 1 mm. b, d–f Scale bars = 0.1 mm



high expression, the longitudinally polarized growth were completely inhibited in transgenic *Arabidopsis* (Matsuoka et al. 1993). The expression of *D3* was found significantly increased in the *htd-1* mutant compared to Nanjing 6 plants, while that of *D10* in the *htd-1* mutant was only slightly higher than in Nanjing 6. In contrast, both *HTD1* and *D10* exhibited lower expression in the *d3* mutant than in the wild-type plants (Zou et al. 2006). Inconsistent with

the report by Zou et al. (2006), levels of *D10* transcripts were substantially increased in *d3* and *d14* mutants, while *D3* and *HTD1* expression was unaltered (Arite et al. 2007). It may attribute to different plant tissues for RT-PCR analysis. In agreement with previous report by Arite et al. (2007), the mutation of the *D88* gene in *d88* caused the increased mRNA level of *D10*, a proposed limiting factor in the control of shoot branching in rice. It appears

conceivable that a feedback mechanism that regulates *D10* expression reacts to a lesion in *D88*. However, in contrast to the report on *d14* by Arite et al. (2007), *HTD1* transcription was enhanced in stem base of the *d88* mutant. It may be explained by weakened function of *D88* in the *d14* mutant.

D88 is a novel esterase regulating plant development

To date for rice, esterase has mostly been implicated in plant–pathogen interactions (Wäspie et al. 1998). A methyl jasmonate esterase identified in potato related to plant defense and an ethylene induced cell wall hydrolase during abscission in orange have little similarity to D88 (Fridman et al. 2005; Zhong et al. 2001). However, a variety of these isozymes found throughout plant have developed to perform specific metabolic reaction. Gene expression of esterase isozyme in alfalfa root was consistent with the creeping root character (Gao et al. 1994). PME (EC 3.1.1.11) catalyzed the hydrolysis of methylester groups of cell wall pectins in seeds of yellow cedar and its high activity coincided with dormancy breakage and germination (Ren and Kermodé 2000). *GIDI* gene, isolated from rice GA-insensitive dwarf mutant *gid1*, was characterized to encode an unknown protein with high similarity to the hormone-sensitive lipase, a soluble receptor located in nuclei mediating GA signaling (Ueguchi-Tanaka et al. 2005). More recently, rice *EXTRA GLUME1* gene encoding a putative lipase was cloned and confirmed to specify empty-glume fate and floral meristem determinacy (Li et al. 2008).

Our study thus demonstrates that D88, a novel putative esterase, plays an important role in the regulation of cell growth and organ development that alters drastically rice plant architecture. Clearly, *D88* represents a category of genes that affect plant architecture. Not fully restoration for the plant height in complementation test possibly due to competition for the unknown substrate in transgenic lines. Recently, strigolactone was discovered by two research groups as a new hormone inhibiting shoot branching and regulating above-ground plant architecture in pea and rice (Gomez-Roldan et al. 2008; Umehara et al. 2008). Strigolactones are compounds thought to be derived from carotenoids and are known to trigger the germination of parasitic plant seeds and stimulate symbiotic fungi (Akiyama et al. 2005; Matusova et al. 2005). Although our indirect evidence suggested D88 linking to the MAX/RMS/D pathway, whether D88 participate in strigolactones biosynthesis is yet to be determined directly by measurement of the hormone content. Nevertheless, further identification of the substrate for D88 should enhance our understanding of molecular mechanisms underlying plant development and possibly lead to the characterization of a new pathway regulating plant architecture.

**Acknowledgments** This work was supported by grants from the Ministry of Science and Technology of China (2006AA10A102), the Chinese Academy of Sciences (KSCW2-YW-N-024), and the National Natural Science Foundation of China (Grant Nos. 30400255 and 30821004). We thank Prof. Gao Xiaoyan at Institute of Plant Physiology and Ecology in Shanghai for histological analysis of stem base sections of Lansheng and *d88*. We are grateful to Ms. Yan Honglan at China National Rice Research Institute for photograph, Dr. Huang Xuehui at National Center for Gene Research for critical reading of the manuscript.

## References

- Akiyama K, Matsuzaki K, Hayashi H (2005) Plant sesquiterpenes induce hyphal branching in arbuscular mycorrhizal fungi. *Nature* 435:824–827
- Arite T, Iwata H, Ohshima K, Maekawa M, Nakajima M, Kojima M, Sakakibara H, Kyojuka J (2007) *DWARF10*, an *RMS1/MAX4/DAD1* ortholog, controls lateral bud outgrowth in rice. *Plant J* 51: 1019–1029
- Felsenstein J (1985) Confidence limits on phylogenies: an approach using the bootstrap. *Evolution* 39:783–791
- Fontana F (2007) Isolation of differentially expressed transcripts—after treatment of *platanus acerifolia* leaves with cerato-platanin, a multi-functional protein from *ceratocystis platani*. *J Plant Pathol* 89(Suppl):S3
- Fridman E, Wang J, Iijima Y, Froehlich JE, Gang DR, Ohlrogge J, Pichersky E (2005) Metabolic, genomic, and biochemical analyses of glandular trichomes from the wild tomato species *Lycopersicon hirsutum* identify a key enzyme in the biosynthesis of methylketones. *Plant Cell* 17:1252–1267
- Gao Z, Wang P, Hong F, Xie X (1994) Change of esterase isozyme and endogenous hormone in root system and ontogenesis of creeping-rooted character in alfalfa. *Acta Agrestia Sinca* 2:1–11
- Gomez-Roldan V, Fermas S, Brewer PB, Puech-Pagès V, Dun EA, Pillot JP, Letisse F, Matusova R, Danoun S, Portais JC, Bouwmeester H, Bécard G, Beveridge CA, Rameau C, Rochange SF (2008) Strigolactone inhibition of shoot branching. *Nature* 455:189–194
- Hiei Y, Ohta S, Komari T, Kumashiro T (1994) Efficient transformation of rice (*Oryza sativa* L.) mediated by *Agrobacterium* and sequence analysis of the boundaries of the T-DNA. *Plant J* 6:271–282
- Hubbard L, McStern P, Doebley J, Hake S (2002) Expression patterns and mutant phenotype of *teosinte branched1* correlate with growth suppression in maize and teosinte. *Genetics* 162: 1927–1935
- Ishikawa S, Maekawa M, Arite T, Ohnishi K, Takamura I, Kyojuka J (2005) Suppression of tiller bud activity in tillering dwarf mutants of rice. *Plant Cell Physiol* 46:79–86
- Jefferson RA, Kavanagh TA, Bevan MW (1987) GUS fusions: beta-glucuronidase as a sensitive and versatile gene fusion marker in higher plants. *EMBO J* 6:3901–3907
- Kishimoto N, Shimosaka E, Matsuura S, Saito A (1992) A current RFLP linkage map of rice alignment of molecular map with the classical map. *Rice Genetics Newslett* 9:118–124
- Lander ES, Green P, Abrahamson J, Barlow A, Daly MJ, Lincoln SE, Newberg L (1987) Mapmaker: an interactive computer package for constructing primary genetic linkage maps of experimental and natural populations. *Genomics* 1:174–181
- Li X, Qian Q, Fu Z, Wang Y, Xiong G, Zeng D, Wang X, Liu X, Teng S, Hiroshi F, Yuan M, Luok D, Han B, Li Y (2003) Control of tillering in rice. *Nature* 422:618–621
- Li H, Xue D, Gao Z, Yan M, Xu W, Xing Z, Huang D, Qian Q, Xue Y (2008) A putative lipase gene *EXTRA GLUME1* regulates both

- empty-glume fate and spikelet development in rice. *Plant J* 57: 593–605
- Lin H, Wang R, Qian Q, Yan M, Meng X, Fu Z, Yan C, Jiang B, Su Z, Li J, Wang Y (2009) DWARF27, an iron-containing protein required for the biosynthesis of strigolactones, regulates rice tiller bud outgrowth. *Plant Cell*
- Matsuoka M, Ichikawa H, Saito A, Tada Y, Fujimura T, Kano-Murakami Y (1993) Expression of a rice homeobox gene causes altered morphology of transgenic plants. *Plant Cell* 5:1039–1048
- Matusova R, Rani K, Verstappen FW, Franssen MC, Beale MH, Bouwmeester HJ (2005) The strigolactone germination stimulants of the plant-parasitic *Striga* and *Orobancha* spp. are derived from the carotenoid pathway. *Plant Physiol* 139:920–934
- Page RDM (1996) TREEVIEW: an application to display phylogenetic trees on personal computers. *Comput Appl Biosci* 12:357–358
- Qian Q, Li YH, Zeng D, Teng S, Wang Z, Li X, Dong Z, Dai N, Sun L, Li J (2001) Isolation and genetic characterization of a fragile plant mutant rice (*Oryza sativa* L.). *Chin Sci Bull* 46:2082–2085
- Reintanz B, Lehnen M, Reichelt M, Gershenzon J, Kowalczyk M, Sandberg G, Godde M UhlR, Palme K (2001) *Bus*, a bushy *Arabidopsis* CYP79F1 knockout mutant with abolished synthesis of short-chain aliphatic glucosinolates. *Plant Cell* 13:351–367
- Ren CW, Kermod AR (2000) An increase in pectin methyl esterase activity accompanies dormancy breakage and germination of yellow cedar seeds. *Plant Physiol* 124:231–242
- Saitou N, Nei M (1987) The neighbor-joining method: a new method for reconstructing phylogenetic trees. *Mol Biol Evol* 4:406–425
- Takeda K (1977) Internode elongation and dwarfism in some gramineous plants. *Gamma Field Sym* 16:1–18
- Takeda T, Suwa Y, Kitano H, Ueguchi-Tanaka M, Ashikari M, Matsuoka M, Ueguchi C (2003) The *OsTB1* gene negatively regulates lateral branching in rice. *Plant J* 33:513–520
- Ueguchi-Tanaka M, Ashikari M, Nakajima M, Itoh H, Katoh E, Kobayashi M, Chow TY, Hsing YI, Kitano H, Yamaguchi I, Matsuoka M (2005) *GIBBERELLIN INSENSITIVE DWARF1* encodes a soluble receptor for gibberellin. *Nature* 437:693–698
- Umehara M, Hanada A, Yoshida S, Akiyama K, Arite T, Takeda-Kamiya N, Magome H, Kamiya Y, Shirasu K, Yoneyama K, Kyojuka J, Yamaguchi S (2008) Inhibition of shoot branching by new terpenoid plant hormones. *Nature* 455:195–200
- Wadsworth GJ, Redinbaugh MG, Scandalios JG (1988) A procedure for the small-scale isolation of plant RNA suitable for RNA blot analysis. *Analyt Biochem* 172:279–283
- Wang Y, Li J (2008) Molecular basis of plant architecture. *Annu Rev Plant Biol* 59:253–279
- Ward SP, Leyser O (2004) Shoot branching. *Curr Opin Plant Biol* 7: 73–78
- Wäspie U, Misteli B, Hasslacher M, Jandrositz A, Kohlwein SD, Schwab H, Dudler R (1998) The defense-related rice gene *Pir7b* encodes an  $\alpha/\beta$  hydrolase fold protein exhibiting esterase activity towards naphthol AS-esters. *Eur J Biochem* 254:32–37
- Yan H, Saika H, Maekawa M, Takamura I, Tsutsumi N, Kyojuka J, Nakazono M (2007) Rice tillering dwarf mutant *dwarf3* has increased leaf longevity during darkness-induced senescence or hydrogen peroxide-induced cell death. *Genes Genet Syst* 82: 361–366
- Zhong G, Goren R, Riov J, Sisler EC, Holland D (2001) Characterization of an ethylene-induced esterase gene isolated from *Citrus sinensis* by competitive hybridization. *Physiol Plantarum* 113: 267–274
- Zou J, Chen Z, Zhang S, Zhang W, Jiang G, Zhao X, Zhai W, Pan X, Zhu L (2005) Characterizations and fine mapping of a mutant gene for high tillering and dwarf in rice (*Oryza sativa* L.). *Planta* 222:604–612
- Zou J, Zhang S, Zhang W, Li G, Chen Z, Zhai W, Zhao X, Pan X, Xie Q, Zhu L (2006) The rice *HIGH-TILLERING DWARF1* encoding an ortholog of *Arabidopsis* MAX3 is required for negative regulation of the outgrowth of axillary buds. *Plant J* 48:687–696